SIMULATION ANALYSIS OF THE INFLUENCED MOTION FROM

BALL MASS AND SHAPE IN BASEBALL PITCHING

Yoshiyuki MOCHIZUKI

Multimedia Development Center, Matsushita Electric Industrial Co., Ltd.
1006, Kadoma, Kadoma-shi, Osaka 571-8501 Japan
e-mail: mochik@isl.mei.co.jp

Abstract. *We call the ideal motion generated under the artificial environment like a computer "artificial proficient motion". This paper reports the simulation analysis for upper limb how influence is given to pitching motion from ball mass and shape by using the new simulation method for generating artificial proficient motion. The most important feature of our simulation method is that there is a mechanism of the process for obtaining the proficient motion on a computer. In this paper, at first, we have described the new computer simulation method of generating artificial proficient motion for upper limb during baseball pitching by using the 3-dimensional mathematical model and the optimizing method. Secondly, we have reported the simulation experiment and its consequences for investigating the influence from several types of a ball, in baseball, golf, American football, Basketball and etc., to the pitching motion on one's upper limb by applying our simulation method. From the consequences, we have been able to make clear the property of the influenced motion from ball mass and shape on one's upper limb in viewpoints of dynamics and kinematics.*

1. INTRODUCTION

It is easy to suppose that the pitching motion is influenced from the ball mass and shape. The motive mechanism on the upper limb during baseball pitching has been investigated formerly by using 3-dimensional measurement of a motion in the field of sports biomechanics [1][2][3][4][5][6][12]. It is, however, hard to investigate how it works by using an actual human body because the testee might be injured by the experiments without the knowledge of the influence. Additionally, it is difficult for the testee to execute the quantitative experiment under the same conditions, and it is impossible for the testee to reproduce the same motion completely. The simulation analysis plays the important role in these cases.

In the field of sports, it is possible to consider the proficient skill motion to be the optimizing skill motion under some conditions. We call the ideal proficient skill motion generated under the artificial environment like a computer "artificial proficient motion", and we have dedicated to study the artificial proficient motion for upper limb in baseball pitching [7][8]. In this report, we have mentioned the simulation analysis of the influenced motion from ball mass and shape for several types of a ball with different mass and shape, in baseball, golf, tennis, Japanese baseball, softball, handball, American football, and basketball by using the simulation method for generating artificial proficient motion for upper limb in baseball pitch. We have also discussed the consequences of the simulation experiment in viewpoints of dynamics and kinematics. Our research might be able to provide the new data and the new information about the influence of ball mass and shape to a researcher by using 3-dimensional measurement of a motion mention previously.

2. SIMULATION METHOD

Process Flow

Figure 1 shows the process flow for generating the artificial proficient pitching motion under some conditions of a ball and a human body. At first, the actual pitching motion for someone is captured by DLT (Direct Linear Transformation) method [9]. The captured data is transformed to the time sequence data of joint angles, and they are also utilized to calculate the physical parameter. The inertia tensor of each part of an upper limb and a ball are calculated by numerical integral with approximated curved surfaces. The physical parameter, the ball data about mass and shape, and their inertia tensor are input to the process executing optimizing calculation for upper limb. After the optimizing calculation, the obtained optimizing motion is combined with the original motion of other parts of the body except the upper limb, and then the whole motion for a human body is visualized by the software that we have developed. The data for the optimizing pitching motion is also represented by a graph for analysis.
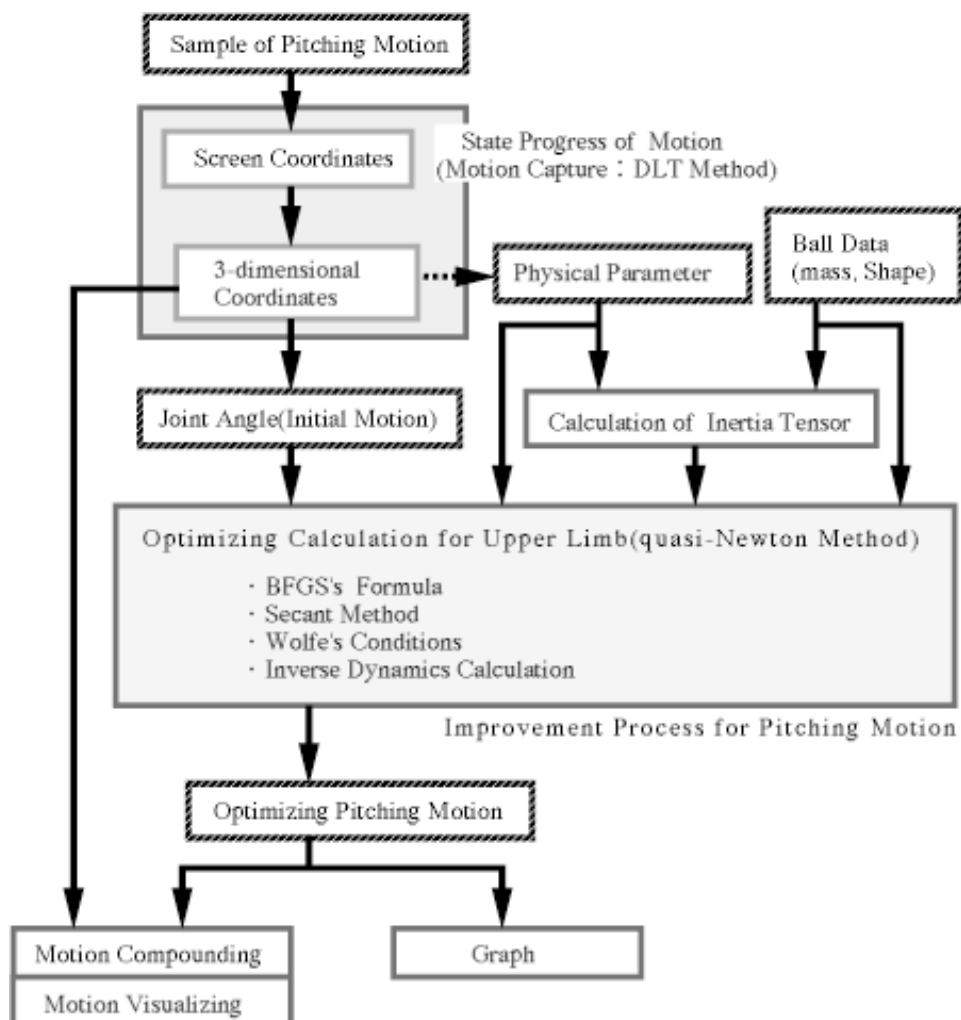

Figure 1: Process Flow for Artificial Proficient Motion
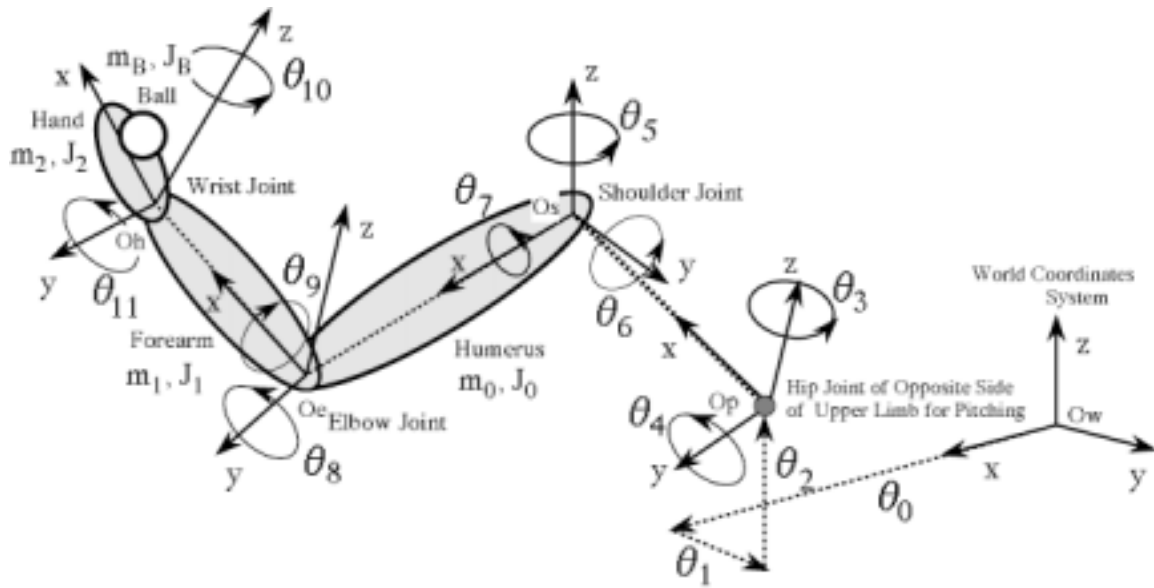
Mathematical Model

Figure 2: Mathematical Model for Upper Limb

Figure 2 indicates our 3-dimensional mathematical model for upper limb that totally has twelve degrees of freedom. Each part of upper limb and a ball is approximated by a rigid body with uniform density. The motion on upper limb is only affected by the trajectory of the shoulder joint on the 3-dimensional space. The trajectory of the shoulder joint can be controlled by five degrees of freedom for the local coordinate system with the origin defined at the hip joint on the opposite side of the upper limb for pitch. These five degree of freedom comprise of three translations for each axis of a world coordinate system and two rotations around the z-axis and the y-axis of the local coordinate system. The upper limb is controlled by the remaining seven degrees of freedom utilized in D-H (Denavit and Hartenberg) representation [10] applied to the local coordinate system for the model, where the x-axis of it coincides with the joint axis. θ_0, …, and θ_4 are variables for controlling the trajectory of the shoulder joint, θ_5 corresponds to horizontal adduction or abduction, θ_6: adduction or abduction, θ_7: internal rotation or external rotation, θ_8: flexion or extension, θ_9: pronation or supination, θ_{10}: radial-flexion or ulnar-flexion, and θ_{11}: flexion or extension, where θ_i: is defined at the i-th local coordinate system.

The model is described by two systems of Lagrange equations that expresses the pitching motion before/after releasing a ball. For example, the system of Lagrange equations before releasing a ball can be represented by the following equations (1), (2), and (3):

$$\tau_i = \sum_{k=0}^{7} \text{trace}\left[\frac{\partial T_7}{\partial \theta_k} J_0 \frac{\partial T_7^T}{\partial \theta_i}\right]\ddot{\theta}_k + \sum_{k=0}^{9} \text{trace}\left[\frac{\partial T_9}{\partial \theta_k} J_1 \frac{\partial T_9^T}{\partial \theta_i}\right]\ddot{\theta}_k$$

$$+ \sum_{k=0}^{11}\left[\text{trace}\left[\frac{\partial T_{11}}{\partial \theta_k} J_2 \frac{\partial T_{11}^T}{\partial \theta_i}\right] + \text{trace}\left[\frac{\partial T_B}{\partial \theta_k} J_B \frac{\partial T_B^T}{\partial \theta_i}\right]\right]\ddot{\theta}_k$$

$$+ \sum_{k=0}^{7}\sum_{l=0}^{7} \text{trace}\left[\frac{\partial^2 T_7}{\partial \theta_l \partial \theta_k} J_0 \frac{\partial T_7^T}{\partial \theta_i}\right]\dot{\theta}_k \dot{\theta}_l + \sum_{k=0}^{9}\sum_{l=0}^{9} \text{trace}\left[\frac{\partial^2 T_9}{\partial \theta_l \partial \theta_k} J_1 \frac{\partial T_9^T}{\partial \theta_i}\right]\dot{\theta}_k \dot{\theta}_l$$

$$+ \sum_{k=0}^{11}\sum_{l=0}^{11}\left[\text{trace}\left[\frac{\partial^2 T_{11}}{\partial \theta_l \partial \theta_k} J_2 \frac{\partial T_{11}^T}{\partial \theta_i}\right] + \text{trace}\left[\frac{\partial^2 T_B}{\partial \theta_l \partial \theta_k} J_B \frac{\partial T_B^T}{\partial \theta_i}\right]\right]\dot{\theta}_k \dot{\theta}_l$$

$$- m_0 g^T \frac{\partial T_7}{\partial \theta_i} r_0 - m_1 g^T \frac{\partial T_9}{\partial \theta_i} r_1 - m_2 g^T \frac{\partial T_{11}}{\partial \theta_i} r_2 - m_B g^T \frac{\partial T_B}{\partial \theta_i} r_B$$

$$\text{where } i=0,1,\cdots,7 \tag{1}$$

$$\tau_i = \sum_{k=0}^{9} \text{trace}\left[\frac{\partial T_9}{\partial \theta_k} J_1 \frac{\partial T_9^T}{\partial \theta_i}\right]\ddot{\theta}_k$$

$$+ \sum_{k=0}^{11}\left[\text{trace}\left[\frac{\partial T_{11}}{\partial \theta_k} J_2 \frac{\partial T_{11}^T}{\partial \theta_i}\right] + \text{trace}\left[\frac{\partial T_B}{\partial \theta_k} J_B \frac{\partial T_B^T}{\partial \theta_i}\right]\right]\ddot{\theta}_k$$

$$+ \sum_{k=0}^{9}\sum_{l=0}^{9} \text{trace}\left[\frac{\partial^2 T_9}{\partial \theta_l \partial \theta_k} J_1 \frac{\partial T_9^T}{\partial \theta_i}\right]\dot{\theta}_k \dot{\theta}_l$$

$$+ \sum_{k=0}^{11}\sum_{l=0}^{11}\left[\text{trace}\left[\frac{\partial^2 T_{11}}{\partial \theta_l \partial \theta_k} J_2 \frac{\partial T_{11}^T}{\partial \theta_i}\right] + \text{trace}\left[\frac{\partial^2 T_B}{\partial \theta_l \partial \theta_k} J_B \frac{\partial T_B^T}{\partial \theta_i}\right]\right]\dot{\theta}_k \dot{\theta}_l$$

$$- m_1 g^T \frac{\partial T_9}{\partial \theta_i} r_1 - m_2 g^T \frac{\partial T_{11}}{\partial \theta_i} r_2 - m_B g^T \frac{\partial T_B}{\partial \theta_i} r_B$$

$$\text{where } i=8,9 \tag{2}$$

$$\tau_i = \sum_{k=0}^{11}\left[\text{trace}\left[\frac{\partial T_{11}}{\partial \theta_k} J_2 \frac{\partial T_{11}^T}{\partial \theta_i}\right] + \text{trace}\left[\frac{\partial T_B}{\partial \theta_k} J_B \frac{\partial T_B^T}{\partial \theta_i}\right]\right]\ddot{\theta}_k$$

$$+ \sum_{k=0}^{11}\sum_{l=0}^{11}\left[\text{trace}\left[\frac{\partial^2 T_{11}}{\partial \theta_l \partial \theta_k} J_2 \frac{\partial T_{11}^T}{\partial \theta_i}\right] + \text{trace}\left[\frac{\partial^2 T_B}{\partial \theta_l \partial \theta_k} J_B \frac{\partial T_B^T}{\partial \theta_i}\right]\right]\dot{\theta}_k \dot{\theta}_l$$

$$- m_2 g^T \frac{\partial T_{11}}{\partial \theta_i} r_2 - m_B g^T \frac{\partial T_B}{\partial \theta_i} r_B \qquad \text{where } i=10,11 \tag{3}$$

In these equations, m_i is the mass, J_i is the matrix of inertia, r_i is the position vector of the barycenter, g is the vector of the gravitational acceleration, and $T_i = A_0 A_1 \ldots A_i$ where A_i is the 4 times 4 matrix that transforms the expression on the i-th local coordinate system to the expression on the i-1-th local coordinate system and A_B is the matrix that transforms the expression on the local coordinate system for the ball to the expression on the 11th local coordinate system. The system of Lagrange equations after releasing a ball can be represented in the same way.

In our mathematical model, we determined that the ball release is executed when the velocity vector of the ball on the hand has the vertical component to the under direction and the horizontal velocity of it takes the maximum value. The trajectory and the velocity of the ball after releasing are calculated by Newton equation with considering the frictional force from air in proportion to the velocity.

Objective Function

We have determined the following equation (4) as the objective function for generating the artificial proficient pitching motion.

$$E\ (\Theta(t)) = W_0 \int (\tau_5^2 + \tau_6^2 + \cdots + \tau_{11}^2)\ dt$$
$$+ W_1 \int [(d\tau_5/dt)^2 + (d\tau_6/dt)^2 + \cdots + (d\tau_{11}/dt)^2] dt$$
$$+ W_2 \ (\text{Penalty for Ball Velocity})$$
$$+ W_3 \ (\text{Penalty for Joint Movability})$$
$$+ W_4 \ (\text{Penalty for Joint Torque})$$

(4)

where $\Theta(t) = (\theta_5(t), \ldots, \theta_{11}(t)$ and W_i is the weight coefficient.

The objective function is one of the most important thing for our simulation method in the meaning that it determines the feature and the property of the proficient motion. The keywords of "wasteless" and "smooth" are often used when the superiority of pitching motion is criticized. The first term of the equation (4) is the total torque described by L2 norm type expression, and it can be expected that minimizing the first term corresponds to "wasteless" in the sense of minimizing the area enclosed by the torque function. The second term of the equation (4) represents the total torque derivatives described by L2 norm type expression, and minimizing the second term corresponds to "smooth" in the sense that the sudden occurrences or changes of the torque function exist as little and/or few as possible in the motion. The second term also corresponds to the hypothesis of the minimum torque-change model [11]. The third term of the equation (4) constrains the motion space by the necessary velocity as baseball pitch, and the fourth term and the fifth term restricts the motion space as human motion. The weight coefficient of the objective function is determined by the way such that calculating the value v_0 of the first term of equation(4) when $W_0=1$ for an initial motion, and then the ratio of v_0 to each value of the second term, the third term, the fourth term, and the fifth term is 1: 1: 1: 3: 2.

Optimization

The optimizing calculation for pitching motion is executed to seven degrees of freedom on the upper limb by a quasi-Newton method that consists of BFGS's formula and secant method with Wolfe's condition. BFGS's formula is utilized in the calculation of Hessian for the direction of a search vector, and secant method is executed in order to calculate the length of the search vector. Figure 3 shows the process flow of the optimizing calculation in detail, where $E(\Theta_k(t))$ is the objective function, $\Theta_k(t)$ is the vector of joint functions, and H_k is Hessian in the k-th iteration. The iterative loop is duplicated and, for an initial motion, the inner iterative loop is executed the converging process under the determined weight coefficients calculated by the way mentioned above. The outer iterative loop is carried out after converging the process in the inner iterative loop with changing the initial motion to the converged pitching motion and renewing the weight coefficients according to the same manner mentioned above.
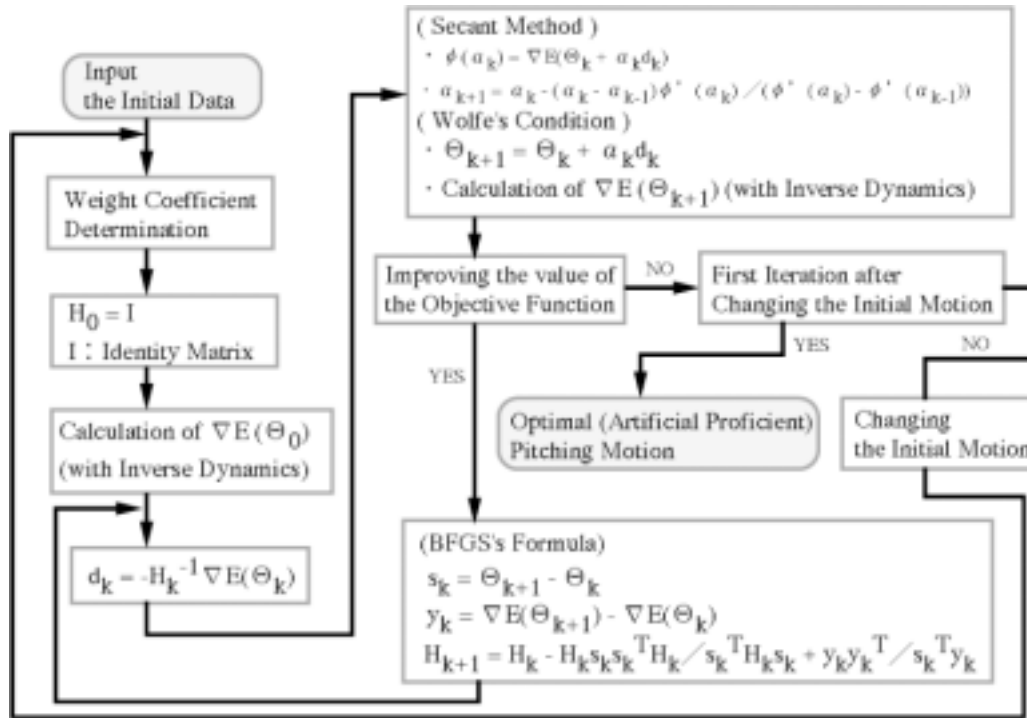
Figure 3: Process Flow for Optimizing Calculation

3. EXPERIMENTS

Method

When an actual human executes pitch for a different ball from a baseball, his pitching motion will be adapted to the ball in stead of his original pitching motion for a baseball. The difference between above two pitching motions is reflected from the influence or the effect that is caused by differences among ball types. Thus, it is meaningless or unrealistic for investigating the influence of ball mass and shape to execute the simulation of changing only ball data for the same pitching motion by the inverse dynamics calculation. In other words, it is necessary for the simulation method to include the mechanism for adapting a motion to a ball type in order to obtain the meaningful and realistic consequences from the simulation experiments. As mentioned above, there is a mechanism for generating the proficient motion on a computer in our simulation method. If the simulation based on our method is executed with changing ball types under the condition with the same initial motion, the same physical parameter, and the same penalties, each converged pitching motions is different from each other since each converged pitching motion is optimized according to each ball type. We can investigate the influence from ball mass and shape by analyzing these differences, and this analysis might be expected to be close to the result from the experiments with using an actual human.

Simulation Condition

The Simulation experiments has been carried out with the same overhand style pitching motion by a professional baseball pitcher as the initial motion. The initial motion has been constructed between the take-back phase and the follow-through phase for 0.860061 second. The simulation has been executed in 0.00286687 second for a time step in the inverse

dynamics calculation. The threshold for the penalty of joint movability on the upper limb has been decided from the medical data. The threshold for the penalty of the load of torque has been determined that the value for a wrist joint is 10.0 Nm and the value for an elbow joint has been 50.0 Nm. The threshold for the ball velocity has been determined 35.0 m/s. The simulation experiments have been executed for the eight kinds of balls such as baseball, golf ball, tennis ball, Japanese baseball, softball, hand ball, American football, and basketball. Table 1 shows the physical data for a human body and Table 2 indicates a ball data in the simulation experiments.

Table 1: Physical Data for Upper Limb

	Mass (kg)	Inertia Tensor H_{xx} (m²kg)	Inertia Tensor H_{yy} (m²kg)	Inertia Tensor H_{zz} (m²kg)	Inertia Tensor H_{xy} (m²kg)	Inertia Tensor H_{yz} (m²kg)	Inertia Tensor H_{zx} (m²kg)
Humerus	1.934663	2.2021262×10^{-3}	$1.21482978 \times 10^{-2}$	$1.24127924 \times 10^{-3}$	1.81309×10^{-5}	-6.0618×10^{-6}	-4.24122×10^{-5}
Forearm	1.127990	8.025930×10^{-4}	5.7933046×10^{-3}	5.9546091×10^{-3}	8.304×10^{-7}	6.455×10^{-7}	9.38436×10^{-5}
Hand	0.3454527	2.081984×10^{-4}	4.655006×10^{-4}	5.049077×10^{-4}	-1.5749×10^{-6}	-2.3634×10^{-6}	-1.19011×10^{-5}

Table 2: Ball Data

	Mass (g)	Radius (cm)	Volume (cm³)	Density (g/cm³)	Inertia Tensor H_{xx} (m² kg)	Inertia Tensor H_{yy} (m² kg)	Inertia Tensor H_{zz} (m² kg)
Baseball	141.8	3.630	200.36	0.7077	7.4739×10^{-5}	7.4739×10^{-5}	7.4739×10^{-5}
Golf	45.92	2.113	39.517	1.162	8.2040×10^{-6}	8.2040×10^{-6}	8.2040×10^{-6}
Tennis	57.59	3.255	144.36	0.3987	2.4397×10^{-5}	2.4397×10^{-5}	2.4397×10^{-5}
Japanese Baseball	136.0	3.600	195.43	0.6959	7.0502×10^{-5}	7.0502×10^{-5}	7.0502×10^{-5}
Softball	191.4	4.775	456.05	0.4197	1.7450×10^{-4}	1.7450×10^{-4}	1.7450×10^{-4}
Handball	450.0	9.390	3468.1	0.1298	1.5871×10^{-3}	1.5871×10^{-3}	1.5871×10^{-3}
American Football	425.0	14.30 / 8.500	2733.0	0.1555	1.4867×10^{-3}	1.0849×10^{-3}	1.4867×10^{-3}
Basketball	625.0	12.18	7568.9	0.08258	3.7060×10^{-3}	3.7060×10^{-3}	3.7060×10^{-3}

4. RESULTS

Figure 4 shows the converged pitching motions for each ball type in cases of baseball, golf, American football, and basketball from the left up side with the trajectory surface of a hand in black curves and lines. In cases of baseball, golf, Japanese baseball, and softball, each figure of the pitching motion has resembled each other, and in cases of handball, American football,

and basketball, each figure of the pitching motion has resembled each other. The difference between two groups has been seen the twisted part on the hand trajectory after the loop part at the middle. The loop part on the hand trajectory has been getting smaller with a ball getting heavier.
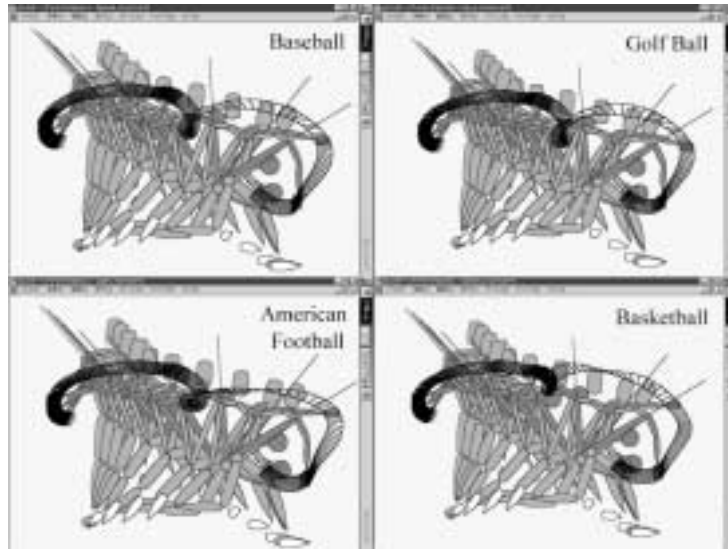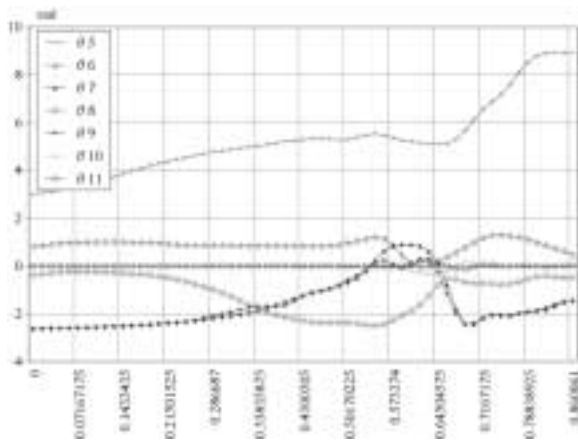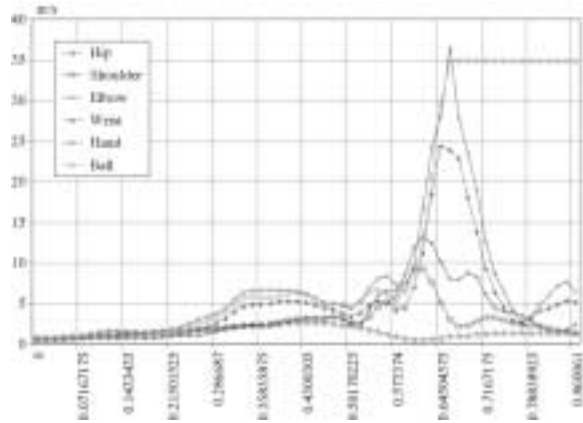

Figure 4: Converged Pitching Motion

Graph 1 to 3 show the graph for joint angles, the graph of the velocity for each joint and a ball, and the graph of the torque at each joint in the case of baseball. Graph 1 shows the quantitative data for joint angles for Figure 4 concretely. Graph 4 to 6 show the graphs of the velocity for each joint, the end of hand, and a ball in cases of handball, American football, and basketball. As Compared with Graph 2, there is the overtaking phenomenon between the hand velocity and the ball velocity in the acceleration phase in Graph 4 to 6. The overtaking phenomenon has not seen in other cases of golf, Japanese baseball, and softball. It is considered that the overtaking phenomenon related with the ball size rather than the ball mass. In the case that the ball size is bigger than baseball, like American football, hand ball, and basket ball, the hand velocity is much slower than ball velocity. In the case of the smaller ball, like golf ball, the hand velocity is faster than the ball velocity. It is caused that the distance between the hand and the center of a ball is bigger or smaller than in the case of baseball. Graph 7 to 13 show the graphs of joint torque in cases of golf ball, tennis ball, Japanese baseball, softball, handball, American football, and basketball. From Graph 3 and 8 to 10, the torque graphs in the cases of tennis ball, Japanese baseball, and softball resembles the torque graph in the case of baseball. From Table 2, the ball density and inertia tensor in those cases resembles each other where, in the case of softball, these properties are intermediate numerically. The peak torque values in the case of golf ball are unexpectedly big in comparison with its mass from Graph 7. Inversely, the peak torque values in the cases of hand ball and American football are unexpectedly small in comparison with their mass from Graph 11 and 12. The consequence related with the above matter has been reported [12] from the experiments by using an actual human with 3-dimensional measurement of a motion. It seems that this difference also relates with the ball density and inertia tensor because these values are much different among them. It seems that there is the limit of mass because, in the case of basketball, the peak torque values are much bigger than that of other cases, especially,
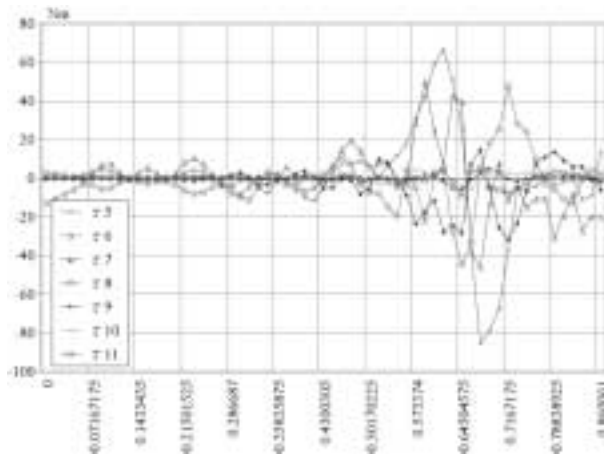
in the rotation torque from Graph 13. However, there is no simple relation, for example, that the peak torque value is getting bigger in proportion to mass.
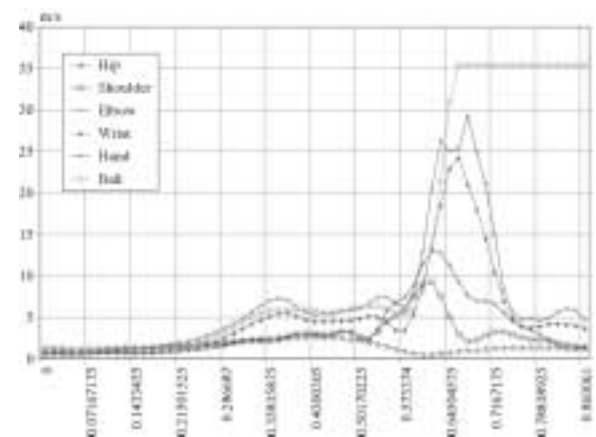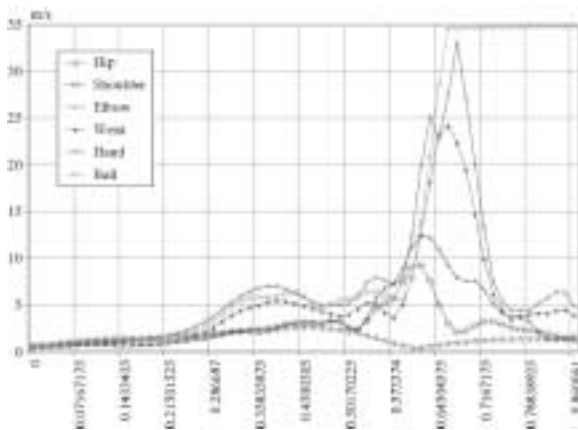
Graph 1: Joint Angle (Baseball)
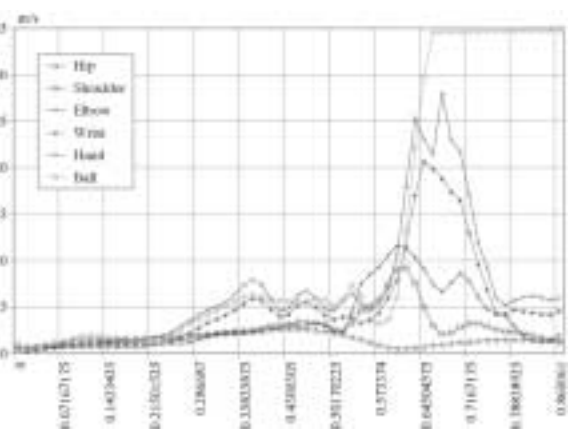
Graph 2: Velocity (Baseball)
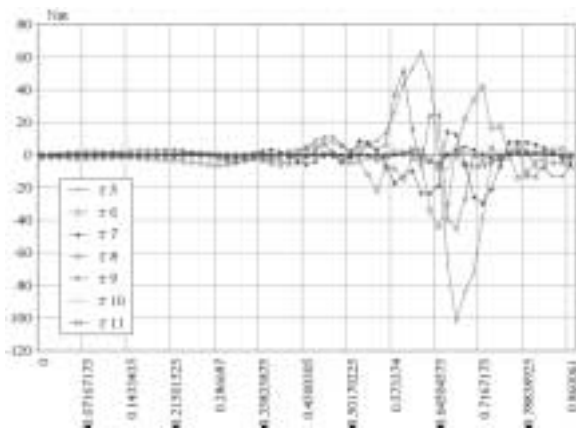
Graph 3: Joint Torque (Baseball)

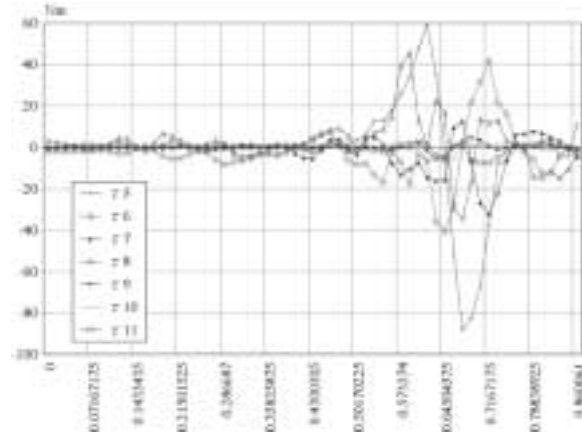**Graph 4: Velocity (Handball)**
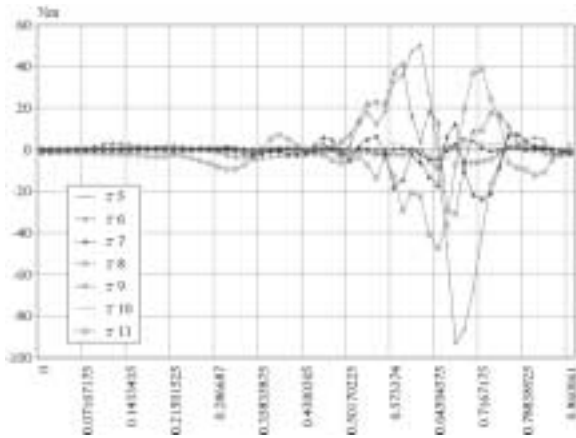
Graph 5: Velocity (American Football)

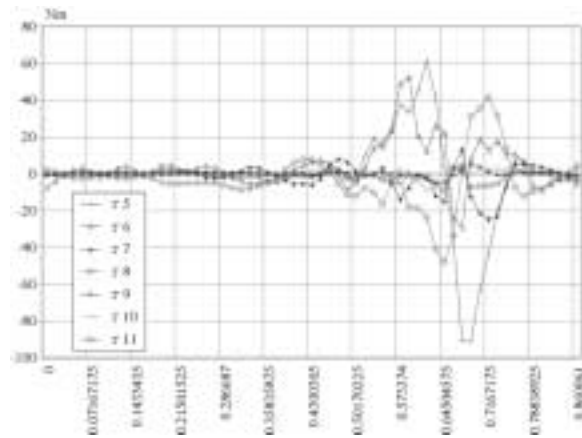**Graph 6: Velocity (Basketball)**
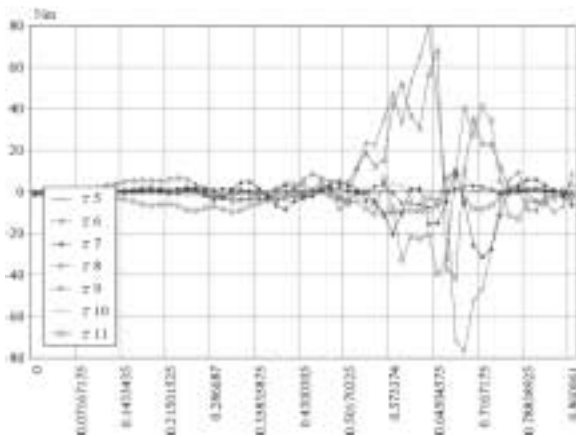
Graph 7: Joint Torque (Golf)

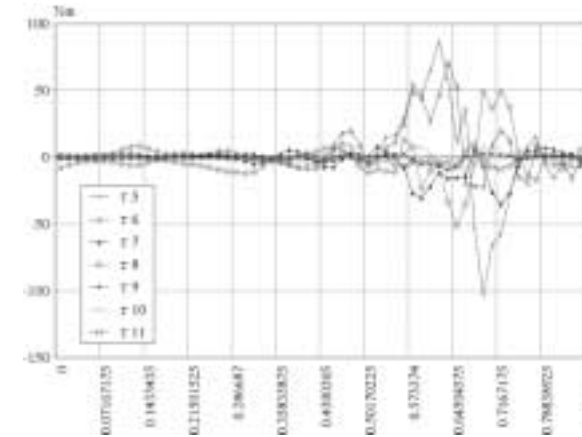

Graph 8: Joint Torque (Tennis)

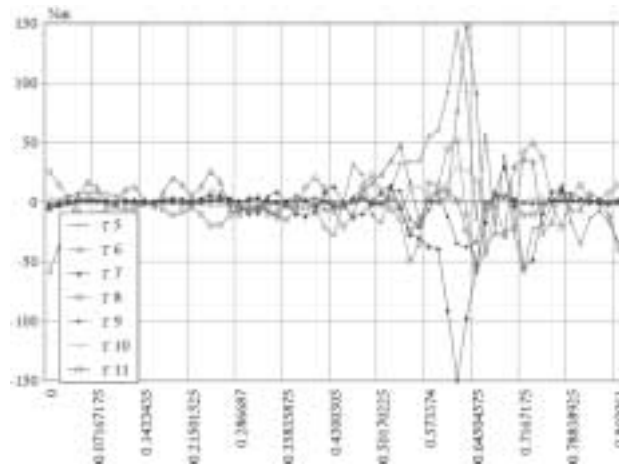**Graph 9: Joint Torque (Japanese Baseball)**

Graph 10: Joint Torque (Softball)

Graph 11: Joint Torque (Handball)

Graph 12: Joint Torque (American Football)

Graph 13: Joint Torque (Basketball)

5. DISCUSSION

From the above results, it can be considered that we can classify these influenced motions generated by our simulation for 8 kinds of balls to following two groups and its boundary:

Group (I): Baseball, Golf ball, Tennis ball, Japanese
baseball,

Group (II) : Handball, American football,
Basketball,

Boundary of (I) and (II)):   Softball.

It seems that these differences are caused from the property of a ball, especially, the ball radius, the density, and the inertia moment. In the section, we discuss the above classification in detail in viewpoint of the kinematics
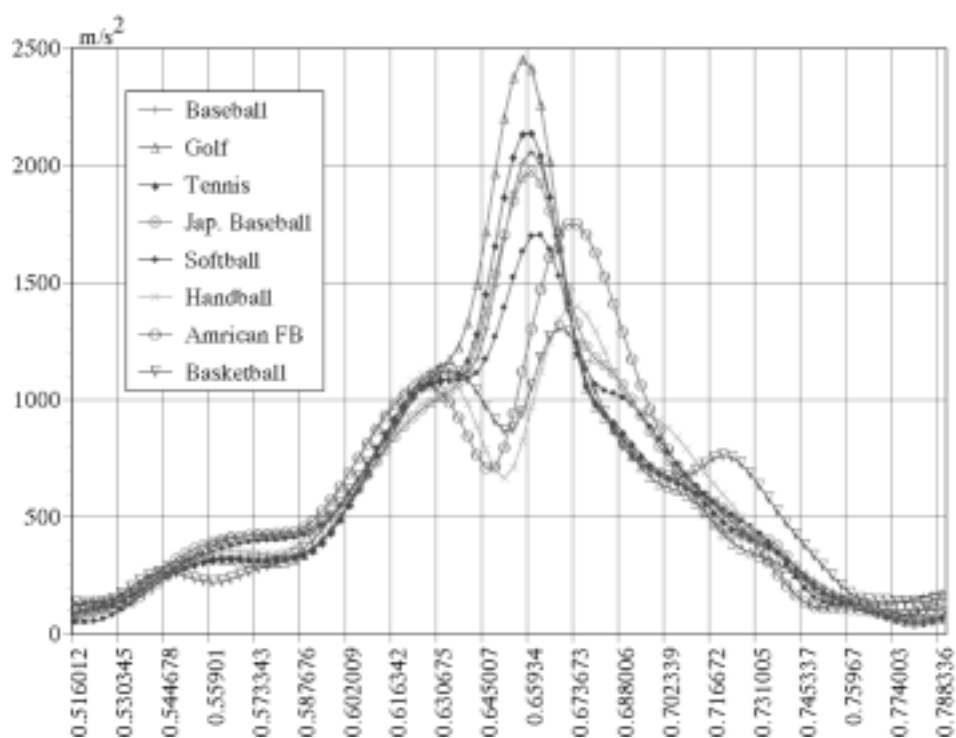
Table 3 indicates the maximum velocity for each joint and a hand with time, the velocity for a ball at release time with release time, and the value obtained from dividing the difference between the maximum velocity for a hand and the velocity of a ball at release by time difference with the value of time interval. From Table 3, it is hard to mention quantitatively, but we can find the coincidence between the sign on the value in the bottom line in Table 3 and the above classification. Since the value is like an acceleration for a hand after release, we can guess that the classification can be also related with the acceleration of a hand in the motion space, and additionally, the jerk (third order derivative).

Graph 14 shows the norm of acceleration vector for a hand between the acceleration phase and the follow-through phase (including the breaking phase) in each case. Graph 15 indicates the norm of jerk vector for a hand between the same time interval. In Graph 14, the difference between above two groups can be seen at the valley on the middle on the time interval and the delay of the peak for the Group (II) . The valley corresponds to the part of the overtaking phenomenon in Graph 4 to 6. We can guess that the valley is generated from the inflection point on the graph of the Group (I) and it can be more clearly seen on Graph 15. In Graph 15, it is considered that the valley between 0.630675s and 0.65934s moves upward.
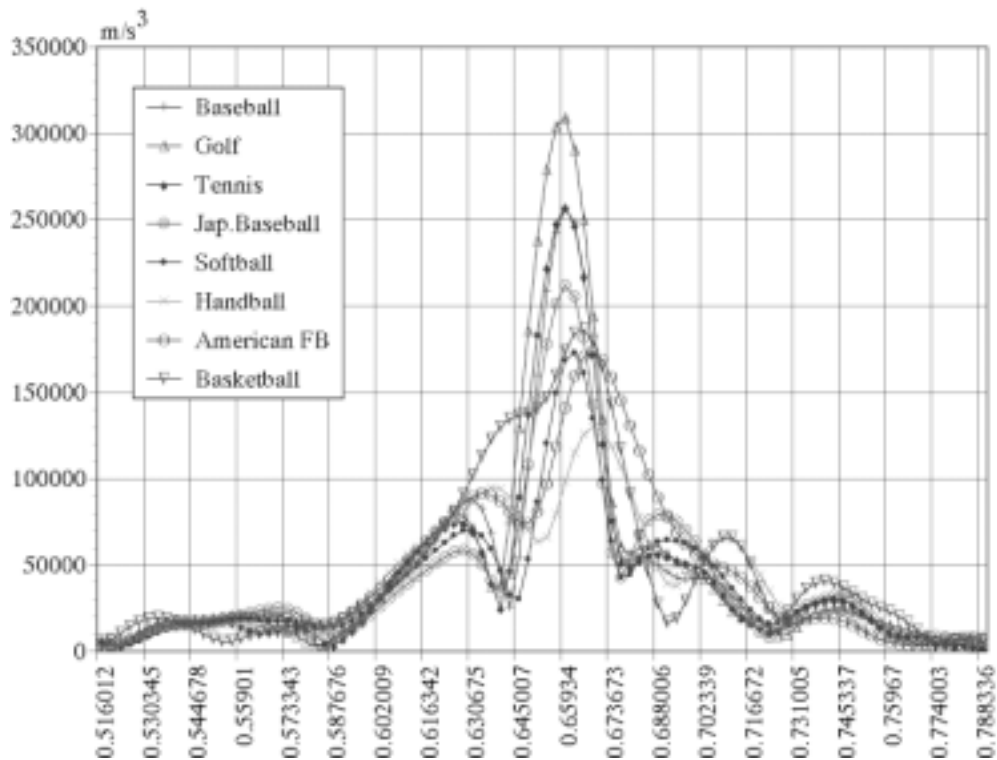
Especially, Graph 14 gives a propriety that the case of softball belongs to the boundary between two groups. The uniqueness in the case of golf ball in the Group (I) is shown at the peak value, and it indicates the uniqueness in the case of basketball in the Group (II) that the graph has the third upward convex part.
.

Table 3: Maximum Velocity

		Baseball	Golf	Tennis	Japanese Baseball	Softball	Handball	American Football	Baketball
Elbow	(m/s)	13.32	13.70	13.48	13.65	13.62	13.08	12.57	11.74
	(sec)	0.6163	0.6163	0.6163	0.6192	0.6192	0.6221	0.6192	0.6077
Wrist	(m/s)	24.76	25.23	24.43	24.69	24.47	24.43	24.33	20.86
	(sec)	0.6507	0.66479	0.6479	0.6507	0.6507	0.6565	0.6565	0.6479
Hand	(m/s)	36.48	39.33	37.09	36.31	33.94	29.32	33.15	28.26
	(sec)	0.6593	0.6564	0.6593	0.6593	0.6593	0.6708	0.6708	0.6708
Ball Release	(m/s)	34.88	34.92	34.99	34.99	35.01	35.40	34.67	34.65
	(sec)	0.6536	0.6536	0.6536	0.6536	0.6536	0.6565	0.6593	0.6536
Hand - Ball Release	(sec)	0.0057	0.0028	0.0057	0.0057	0.0057	0.0143	0.0115	0.0172
	(m/s^2)	-280.7	-1575	-368.4	-231.6	187.7	425.2	132.1	371.5

Graph 14: Acceleration for a Hand

Graph 15: Jerk for a Hand

6. CONCLUSION

In this paper, we have described the simulation analysis for the influenced pitching motion in cases of baseball, golf, tennis, Japanese baseball, softball, handball, American football, and basketball by our simulation method for generating artificial proficient motion in baseball pitch. From the consequence of the simulation experiments, it has been made clear the property and the feature of the influenced motion in viewpoints of dynamics and kinematics. Especially, when the ball size become large, the overtaking phenomenon between the hand velocity and the ball velocity has been observed. With relation to these properties, we have proved that it is possible to classify these motions to two groups and boundary, and we have indicated that the graph of acceleration or jerk for a hand is very useful for the classification.

This research relates to our study of "Artificial Skill" for realization of the collection, the preservation, the reappearance, and the initiation of the proficient skill by the computer technology.

REFERENCES

[1] Michael E.Feltner and Jesus Dapena: "Dynamics of the shoulder and elbow joints of the throwing arm during a baseball pitch", International Journal of Sports Biomechanics, pp235-259, 1986.
[2] Michael E.Feltner and Jesus Dapena: "Three-dimensional interactions in a two-segment kinetic chain. Part 1 : General model", International Journal of Sports Biomechanics, pp403-419, 1989.

[3] Michael E. Feltner: "Three-dimensional interactions in a two-segment kinetic chain. Part 2 : Application to the throwing arm in a baseball pitching", International Journal of Sports Biomechanics, pp420-450, 1989.

[4] S. Sakurai, Y. Ikegami, A. Okamoto, K. Yabe, and S. Toyoshima: "A Three-Dimensional Cinemato-graphic Analysis of Upper Limb Movement During Fastball and Curveball Baseball Pitches", Journal of Applied Biomechanics, 9, pp47-65, 1993.

[5] Rafael F. Escamilla, Glenn S. Fleisig, Steven W. Barrentine, Naiquan Zheng, and James R. Andrews, " Kinematic Comparison of Throwing Different Types of Baseball Pitches", Journal of Applied Biomechanics, 14, pp1-23, 1998.

[6] Steven W. Barrentine, Tomoyuki Matsuo, Rafael F. Escamilla, Glenn S. Fleisig, and James R. Andrews, "Kinematic Analysis of the Wrist and Forearm During Baseball Pitching", Journal of Applied Biomechanics, 14, pp24-39, 1998.

[7] Yoshiyuki Mochizuki, Haruo Amano, Kazushi Tezuka, Tsuyoshi Matsumoto, Shinichi Yamashita, and Koichi Omura, "Computer Simulation for Upper Limb during High Speed Baseball Pitching", Theoretical and Applied Mechanics, Vol.46, pp271-277, 1997.

[8] Yoshiyuki Mochizuki, Tsuyoshi Matsumoto, Kazushi Tezuka, Shinichi Yamashita, Seiji Inokuchi, and Koichi Omura, "Computer Simulation of Generating Artificial Proficient Motion for Upper Limb during Baseball Pitching", Proceedings 1997 International Symposium on Nonlinear Theory and its Applications Vol.1, pp401-404, 1997.

[9] Shapiro, R.: "The direct linear transformation method for three-dimensional cinematography", Res. Quart., 49, pp197-205, 1978.

[10] Denavit, J. and Hartenberg, R.: "A kinematic notation for lower-pair mechanism based on matrices", ASME Journal of Applied Mechanics, 22, pp215-221, 1955.

[11] Uno, Y., Kawato, M., and Suzuki, R.: "Formation and control of optimal trajectory in human multijoint arm movement - minimum torque-change model", Biological Cybernetics, 61, pp89-101, 1989.

[12] Glenn S.Fleisig, Rafael F.Escamilla, James R. Andrews, Tomoyuki Matsuo, Yvonne Satterwhite, and Steve W. Barrentine: "Kinematic and Kinetic Comparison Between Baseball Pitching and Football Passing", Journal of Applied Biomechanics, 12, pp207-224, 1996.